EXPERIMENTAL CYCLIC RESPONSE OF DRY AND WET MASONRY WALLS INCORPORATING CLAY BRICKS AND LIME MORTAR

A.Y. Elghazouli[(1)], D.V. Bompa[(2)], S.A. Mourad[(3)], A. Elyamani[(4)]

[(1)] *Professor, Department of Civil and Environmental Engineering, Imperial College London, UK, a.elghazouli@imperial.ac.uk*
[(2)] *Lecturer, Department of Civil and Environmental Engineering, University of Surrey, UK, d.bompa@surrey.ac.uk*
[(3)] *Professor, Department of Structural Engineering, Cairo University, Egypt, smourad@eng.cu.edu.eg*
[(4)] *Assistant Professor, Department of Archaeological Conservation, Cairo University, Egypt, a_elyamani@cu.edu.eg*

Abstract

This paper investigates the in-plane response of ambient-dry and wet clay-brick/lime-mortar masonry walls under lateral cyclic loading and co-existing compressive gravity load, as well as of square masonry panels under diagonal compression. The properties of the constituent materials were selected to resemble those of existing heritage masonry structures in Historic Cairo. After describing the specimen details and testing arrangements, the main results and observations are provided and discussed. The full load-deformation behaviour of the large-scale wall members is also evaluated, including their ductility and failure modes, and compared with the predictions of available assessment models. It is shown that moisture has a detrimental effect on the main material properties, including the diagonal tension and compression strengths as well as brick-mortar interaction parameters. For the large-scale wall specimens, the wet-to-dry reduction was found to be between 8-11% for the lateral strength and around 10% in terms of ductility. The response of diagonal walls was relatively brittle with a reduction between wet-to-dry strengths of around 33%, suggesting that the reduction ratio is dependent on the compression stress level. Provided that the key moisture-dependent masonry properties are appropriately evaluated, it is also shown that analytical assessment methods can be reliably adapted for predicting the response.

Keywords: masonry walls; lime mortar; clay brick; wet conditions; cyclic loading.

1. Introduction

Seasonal and daily temperature variations produce environmental wet-dry cycling which is recognized to influence the durability and mechanical performance of masonry [1]. A fundamental understanding and quantification of moisture effects on the mechanical properties and structural performance of masonry is hence needed, particularly in the context of seismic assessment of heritage structures [2]. The response of masonry under combined normal force and shear loading is characterised by three independent mechanisms (shear sliding, diagonal cracking and compression crushing) which are assessed from material tests to define limit strength domain of masonry in the form of a shear-precompression diagram [3]. The interface brick-mortar/bed joint response is frequently obtained from small-scale triplet tests [4]. For example, a comparative study on wet and dry triplets has shown that shear strength of wet triplets was about 20% lower on average than those in dry conditions for practical ranges of precompression levels [5].

The diagonal cracking mechanism is characterised by splitting or stepped sliding along the mortar joints, with the ultimate condition depending on the properties and geometry of the brick and mortar as well as their interaction. Although a significant number of representative diagonal panel tests have been reported in the literature [6], such tests on wet conditions seem to be lacking to date. The third mechanism that closes the shear-compression stress space refers to masonry crushing. There is a general agreement that moisture reduces the compressive strength and elastic modulus of masonry, but varies with the mortar properties and brick unit porosity [7]. For example, compressive strengths obtained from tests on prismatic samples were found to be 14% lower for specimens with high moisture in comparison to those in dry conditions, whilst for cylindrical cores this difference was between 13-18% [8].

The ultimate condition of structural masonry is typically evaluated using the shear-compression limit strength domain obtained from small scale tests. Simplified assessment models and codified procedures recognize specific failure modes the develop in masonry components which are broadly divided in flexure and shear [9]. When flexure governs the element behaves like a rigid body with no or minimal diagonal cracking. Damage is concentrated at the edges of the supports, referred to as toe crushing. Shear failures are either in diagonal cracking or sliding. Both existing and newly built structures located in seismic regions need to possess an adequate level of ductility and sufficient structural robustness [10]. The geometry, coupling level and material properties influence not only the strength but also deformation capacity and cyclic degradation of masonry. Cyclic tests on unreinforced dry clay brick – lime mortar masonry squat walls with a height to depth/length ratio h/d=0.7 have shown an essentially elastic response to 0.05% lateral drift, limited deterioration up to 0.1% and an ultimate drift around 0.6% [11].

As mentioned before, water-related problems have been confirmed as a governing factor in degradation of heritage structures and combined with inherent anisotropy would influence the seismic performance of historic masonry, which has rarely been designed with regard to possible effects of lateral loading. This paper presents and experimental programme into the material and structural response of ambient-dry and wet fired clay brick - hydraulic lime mortar masonry elements representative of heritage masonry structures in Historic Cairo. The experimental programme from this paper includes tests on square panels under diagonal compression, triplets in shear, cylindrical cores in compression as well as large-scale walls subjected to gravity load and reverse cyclic or monotonic lateral displacement. The results enable the assessment of the material properties as well as adequacy of available codified provisions.

2. Testing programme

2.1 Material properties and mix designs

Commercial fired clay facing solid bricks with measured sizes of 229×110×66 mm were used for the construction of all specimens. The nominal compressive strength for elements tested parallel to bed face is provided by the manufacturer as 13 MPa, whlist the measured strengths was about 15.5 MPa in both dry and wet conditions, with the latter corresponding to full submersion in water for 48h. From readily available materials, this type of fired-clay bricks has the closest physical and mechanical properties to those from the Mausoleum of Fatima Khatun (Umm al-Salih) built in the 13th century in Cairo, which is assessed in the project. Site surveys indicated that: (i) 'red' bricks (used for the foundation) have a compressive strength (f_b) of about 5.2 MPa and water absorption w_a=27.5%, (ii) 'light brown' bricks have an f_b=14.7 MPa and w_a= 18.1% and (iii) 'dark brown' bricks have an f_b=22.7 MPa and w_a=13.4%. Additionally, the moisture content of both conditioning cases for bricks was assessed. The ambient-dry samples and those submersed in tap water for a minimum of 48h, were dried in an oven for 6h at 60°C and another for 18h at 105°C until the sample mass was relatively constant. The moisture content of ambient-dry bricks was 0.07% by weight (wt.%), and 10.5 wt.% for those submersed in water. These values are in close agreement to those provided by the manufacturer (water absorption $w_a < 10\%$).

Mortars incorporating natural hydraulic lime (NHL) with a binder-to-aggregate ratio of 1:3 were selected for the study as these are typically used for conservation works. An eminently hydraulic binder (NHL5), with a specific gravity of 2.70 was used in the mortars. Mortars with a consistency of 180-200 mm were prepared in the proportions given below, in two batches with different constituents, for comparison purposes in terms of workability and strength. In both cases, for one part of NHL5 lime, 3.25 parts of soft sand were used. In the first batch (A) about 1.20 parts of tap water were added, whilst in the second batch (B) 0.75 parts of tap water and 0.014 parts of plasticiser were mixed. The specific gravity of the sand, typically used for bricklaying and pointing applications, was 2.65 and its water absorption was around 5%. Compressive strengths were determined from compression tests on ambient-dry and wet cubes (50×50×50 mm), and flexural strengths on 25×25×150 prisms. The resulting strengths of the mortars in ambient-dry conditions were between 1.29-2.24 MPa for Batch A samples, whilst for Batch B samples the strengths were between 3.47-5.06 MPa. The

compressive strengths in wet conditions were between 0.58-1.19 MPa for Batch A samples, and these were between 1.62-2.37 MPa for samples from Batch B. An average reduction in elastic modulus in the range of 50% was typically observed due to moisture. Additionally, the moisture content of both conditioning cases for NHL mortar samples was assessed following the same procedure as for the bricks. The moisture content of the lime mortars was 2.54% by weight (wt.%) for ambient-dry samples and 10.80 (wt.%) for those submersed in water.

2.2 Specimen details

2.2.1 Small scale tests

In addition to the large-scale walls of width × height × thickness (b×h×t) = 1910×1300×110 mm, which were tested under combined loading (as illustrated in Fig. 1a and described in the following section), small scale tests on both *wet* and *air-dry* specimens were also carried out to assess the homogenised masonry properties. The small-scale tests included: (i) *diagonal tests* on single leaf square masonry panels of b×h×t = 710×710×110 mm (Fig. 1b), and (ii) *compression tests* on cylindrical masonry cores of 69 mm diameter and 145 mm length, extracted after testing from undamaged areas of the diagonal panels or large-scale walls (Fig. 1c). The specimen reference adopts the format D*X*-*Yz*, where D stands for diagonal panel, *X* indicates the specimen batch (A or B), *Y* represents the conditioning (D for air-dry or W for wet) and z represents the specimen sequence (1, 2, 3, etc.). The panels for diagonal testing (Specimens DA-Dz, DA-Wz, DB-Dz and DB-Wz), as depicted in Fig. 1b, had both horizontal and vertical lime mortar joints with an average thickness of 9 ± 1.5 mm. After the last course of bricks was laid, the specimens were kept in laboratory conditions. Plastic sheets were used to cover the specimens at early curing, and they were tested at 30-35 days.

Prior to testing, the wet specimens were submersed 3/5 of depth in water and were sprinkled with a hose from the top. This procedure ensured even moisture distribution across the specimen. After testing, the wall was dismantled, and samples were extracted to assess the moisture content. After each brick-and-mortar joints were weighed, all components were dried in an oven for 6h at 60°C and for at least 18h at 105°C until the sample mass became largely constant. The moisture distribution results indicated that the same moisture content of 10.7%±0.2 wt was consistently obtained in all nine brick courses. To assess the compressive strength of the masonry, cylinders made of two vertical brick cores, with a mortar joint of about 10 mm in between, were extracted from the diagonal panels and the large walls (Fig. 1c). To ensure a moisture content which is similar to that of the large walls and diagonal panels, the cylinders were submersed for 48h in water. Close inspection of the data obtained from submersing masonry components in water for a period of 24h, indicated that after 3h the masonry specimens had a relatively constant weight. Moreover, the moisture content assessment showed that the moisture was between 10-11%wt.

2.2.1 Large walls under combined loading

From the set of four large-scale specimens of 1910 mm length, 1300 mm height and 110 mm width tested under lateral cyclic loading, two were in *air-dry* and two were in *wet* conditions. All walls were subjected to a nominal gravity load of about 1.0 MPa. The specimen reference adopts the format W*X*-*Y*, where W stands for wall, *X* represents the specimen batch: (A or B), and *Y* represents the conditioning (D for air-dry or W for wet). For example, WA-D is the first test on ambient-dry walls. The masonry walls were constructed on 25 mm thick mild steel plates, prepared with threaded holes (for M20 bolts) for connection to the rig support beam and to facilitate cranage. Stretcher/running bond was used to construct the 16 course high walls. The first course included 8 full bricks per length, whilst each second consecutive course included 7 full bricks and 2 half bricks. To achieve the desired specimen height, the mortar joint thickness was in the range of 8-10 mm. The bricks were laid as received from the manufacturer without any conditioning or soaking in water prior to placing the mortar. Three days before testing, the top transfer beam was placed on the wall and tied to the bottom support steel plate by means of six Ø20 mm threaded ties (see Fig. 2a). Prestressing ensured a slight compression state to the wall while being transported. The plate-wall-beam assembly was then placed on the rig support plate and tied using 6×Ø20 mm bars each side of the wall.

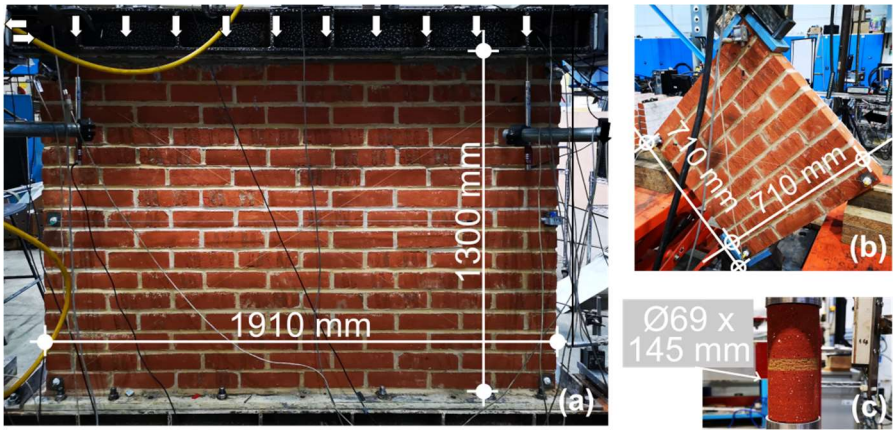

Fig. 1 – Specimen details: a) large scale walls, b) diagonal panels, c) cylindrical cores

For the walls tested under *wet* conditions, the same preparation procedure was followed. To enable wetting through capillary absorption, after the specimens were placed in the testing rig and the prestressing ties were removed, a water tank was built in-place which was connected to the first course of bricks (Fig. 2b). The water tank consisted of 1.0 mm aluminium sheets placed around the perimeter of the wall and tied by means of structural silicone. Tap water was poured into the tank after the silicone reached its setting time. The rising damp resulting from capillary absorption was observed visually and marked on the wall. In addition to the water tank, a pipe/sprinkler system mounted at the top of the wall was manufactured and was used to accelerate the wetting process. To obtain the moisture content of the tested wall and enable direct comparisons with the moisture content of constituent materials as well as the small scale tests described above, twelve samples from the each wet wall (WA-W and WB-W) were taken after testing. The samples were weighed before and after being placed in an oven for 24h at 105°C. The average moisture content was 11.1% by weight which is very similar to the values obtained for brick units and mortar independently. The standard deviation was 0.34%, indicating that the moisture was evenly spread throughout the wall.

2.3 Testing arrangements and instrumentation

The tests on diagonal panels were carried out in a rig which included a main loading transfer frame with a 1000 kN Instron actuator and a connected load cell. As shown in Fig. 3a, the specimens were positioned and loaded through V-shaped supports. The load was applied from the actuator to the top support by means of a hinge. To ensure uniform contact between the loading/support plates and the specimen, a thin timber panel was used. On the other hand, for testing the cylinders in compression, a stiff four-post hydraulic servo-controlled machine with a capacity of 750 kN was used. The cores were tested using the arrangement shown in Fig. 3b. The testing arrangement for the large-scale wall specimens is shown schematically in Fig. 3c. The specimens were directly supported by a 25 mm thick plate and connected by means of prestressed Ø20 mm bolts to a supporting steel beam. The latter was connected to the strong floor by means of 4×Ø33 mm pre-stressing ties to avoid sliding and overturning under lateral loads. At the top of the wall, three 120 kN Enerpac actuators were connected to a steel loading beam and were used to apply the gravity load by means of unidirectional hinges to the specimen through a transfer steel beam. The loads from the vertical actuators were monitored throughout the test to ensure that the axial force applied to the wall was constant.

For the application of the lateral loading, another 250 kN Instron actuator was placed horizontally and connected to the reaction frame. This testing arrangement allowed the top transfer beam to rotate, representing the case of a masonry wall with an intermediate coupling level, behaving largely as a cantilever. After the application of the constant vertical load, corresponding to an axial stress around 1.0 MPa, the lateral deformations were applied based on a pre-defined quasi-static cyclic history. A set of three cycles were applied for each deformation level, corresponding to a drift of 0.025, 0.050, 0.075, 0.10, 0.15, 0.20, 0.25, 0.30, 0.35, 0.40, 0.50, 0.80, 1.0, 1.25, 1.50 (%). The displacement rate and loading procedure were chosen based on

recommendations available in the literature [12]. Lower displacement rates were applied at low drift levels to capture cracking and spalling of mortar and bricks, and this was increased gradually with the drift ratio. A system of steel elements was manufactured to provide out-of-plane stability to the masonry specimen. Two braced cantilevers made of L100×200 sections, with vertical steel rods of Ø50 mm diameter and provided with a double row of steel wheel bearings (44×2.5×37mm), were connected to a stiff frame.

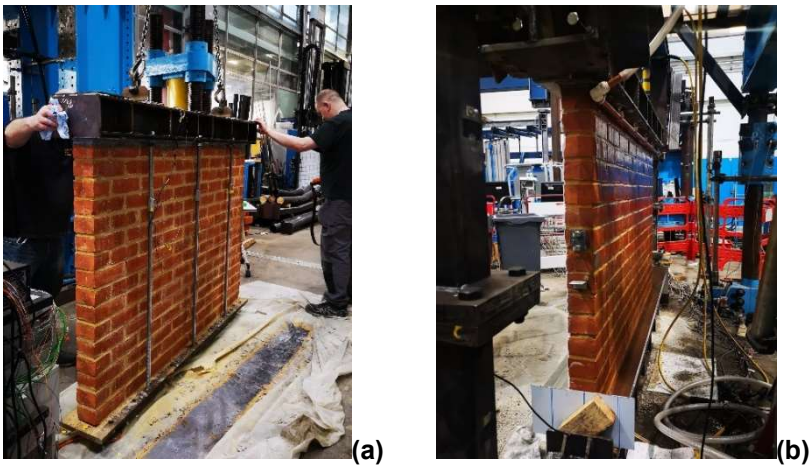

Fig. 2 – Large-scale wall specimen preparation details: a) transportation, b) wetting system

For the diagonal panel tests, besides the machine load and displacement, 2 string pots placed along the two diagonals of the panel, were used. On the other hand, vertical transducers were used to obtain axial deformation of the cylinders tested in compression. The instrumentation of the large-scale walls, apart from the load cells and displacement transducers incorporated within the horizontal and vertical actuators, included 12 additional displacement transducers, 4 string pots of which 2 measured diagonal shear displacement and 2 were inclinometers. A Digital Image Correlation (DIC) system was also employed to record detailed local deformations and strains within the surface of all specimens: large walls, diagonal panels, and cylindrical cores. The DIC system consists of two light-weight CMOS cameras with a USB 3.0 interface for distances up to 25 m. The high sensitivity cameras have a resolution of 2.3 Megapixel at 100 Hz frame rate. After testing, the DIC data were further processed to obtain deformation vector fields. From these, surface strains or deformations were obtained from assigned virtual gauges with various lengths depending on the required measurement.

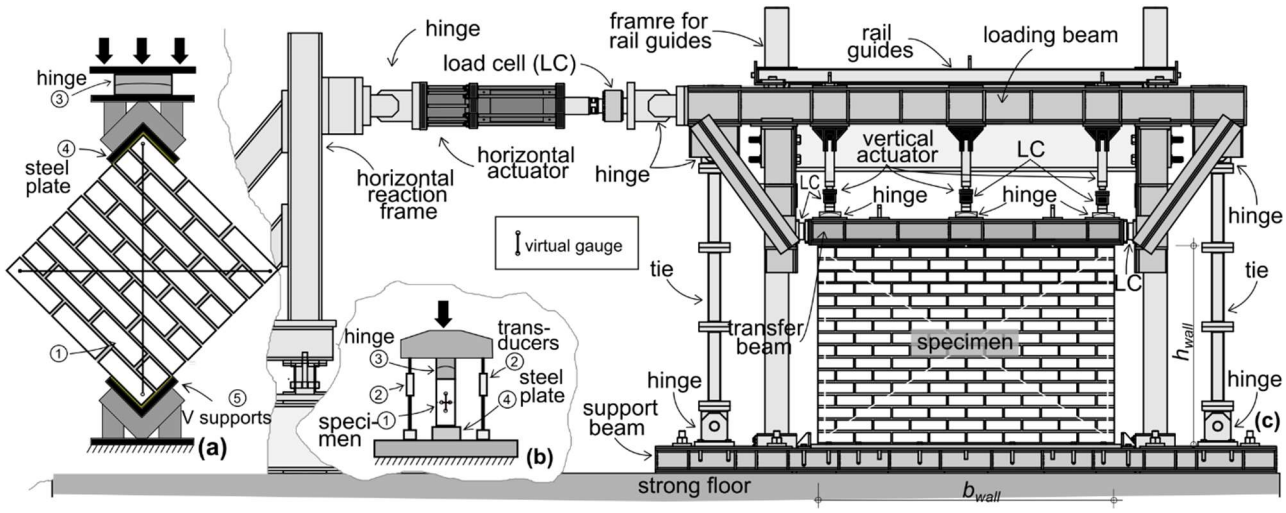

Fig. 3 – Test rigs for: a) diagonal panels, b) cylindrical cores, c) large-scale wall specimens

3. Test results

3.1 Small scale specimens

This section describes the test results of the small-scale specimens illustrated in Fig. 3a,b. These include the tests on the square panels under diagonal compression as well as the cylindrical cores in compression. Fig. 4 depicts the average stress-strain behaviour obtained from the tested panels, whilst Fig. 5 illustrates the typical crack patterns at failure for selected elements. In the diagonal panel tests, the ultimate condition occurs when the principal tensile stresses perpendicular to the compressed strut reaches the maximum tensile strength of the masonry. The shear stress $\tau_{d,test,u}$ was determined by dividing P×cos(α) by 0.5×(b+h) ×t×n, where P is the applied load and α is the angle between the panel diagonal and horizontal axis, parallel to the bed joint. The parameters b, h and t are the panel width, height and thickness, respectively, whilst n is a factor which depends on the perforations (n=1 for solid bricks). The shear strain γ, also referred to as angle of deformation, is the sum of the absolute vertical and horizontal strains, ε_v and ε_h, respectively.

The strain values were obtained from full-field DIC measurements using a virtual gauge of 900 mm length as shown in Fig. 3a. The peak shear stress $\tau_{d,test,u}$ and the shear stiffness G are given in Table 1. The shear stiffness G was evaluated within the elastic regime, corresponding to 10-40% of the ultimate capacity. As indicated by the results in Fig. 4 and Table 1, a direct comparison between the average stress-strain of dry and wet specimens, shows that the moisture reduced both the stiffness and the specimen strength, albeit with different extents in the two batches. On average, the shear stiffness and strength of the wet specimens was reduced by about 35.8% and 28.0%, respectively, compared to the corresponding dry panels. Apart from the significant inherent variability in the bond properties of such low strength lime mortars, the notable differences between the results obtained from the two batches may also be attributed to the influence of the extent of binding water on the microstructural characteristics including pore sizes and pore pressures.

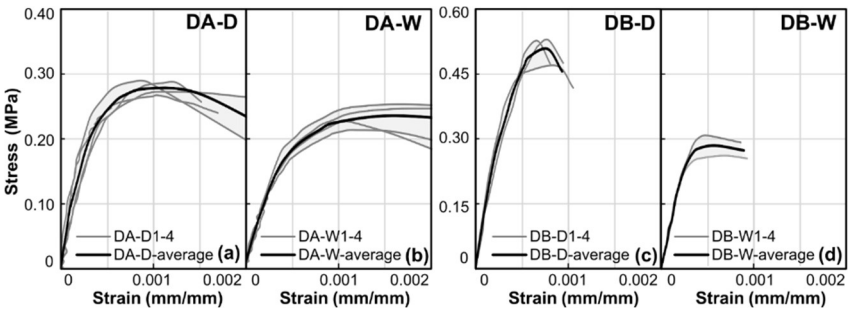

Fig. 4 – Main results for the diagonal panel tests: a) DA-D, b) DA-W, c) DB-D, d) DB-W

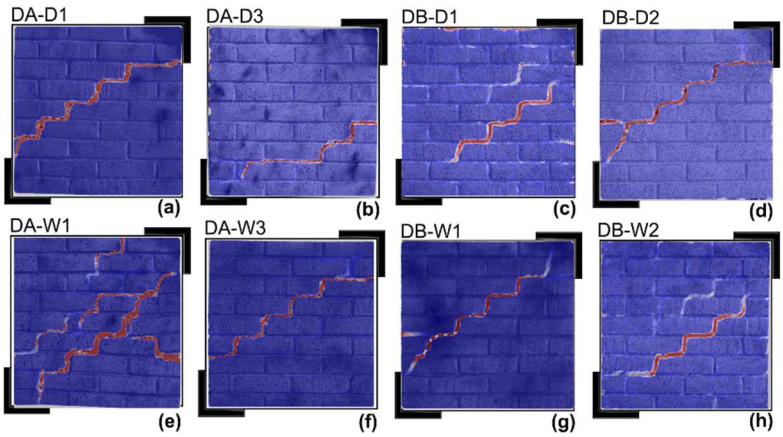

Fig. 5 – Failure patterns for Specimen: a) DA-D1, b) DA-D3, c) DB-D1, d) DB-D2, e) DA-W1, f) DA-W3, g) DB-W1, h) DB-W2

Table 1 – Main results from diagonal panel tests

Speci-mens	n	P_u (kN)	$\tau_{d,test,u}$ (MPa)	G (MPa)	f_m (MPa)	Speci-mens	n	P_u (kN)	$\tau_{d,test,u}$ (MPa)	G (MPa)	f_m (MPa)
DA-D	4	26.9± 2.3	0.28± 0.01	661± 150	5.21± 0.11	DA-W	4	23.5± 2.3	0.24± 0.02	402± 42	4.36± 0.71
DB-D	3	51.1± 2.7	0.51± 0.04	1410± 230	6.08± 0.49	DB-W	2	29.0± 3.54	0.29± 0.03	953± 52	4.87± 0.19

On the other hand, the results of the compression tests on cylindrical masonry cores can be used to evaluate the uniaxial response without the influence of shear. The response of cylinders in compression exhibits a typical brittle response with significant softening immediately after the peak. Close inspection on the stress-strain (σ-ε) curves and the results in Table 1 and 2, it can be observed that the compression strength f_m is notably influenced by the moisture. The wet specimens had, on average, the stiffness and strength of reduced by about 13.6% and 13.3%, respectively, compared to the corresponding dry counterparts, with different extents in the two batches as observed before for the diagonal panels.

3.2 Large scale wall tests

This section describes the main test results from the four large-scale cyclic tests as shown in Fig. 1a and 3c. These included two dry walls (WA-D and WB-D) and two wet walls (WA-W and WB-W). As mentioned above, these specimens were subjected to an initial gravity load of about 1.0 MPa and increasing lateral displacements. The lateral load versus drift (P-Δ) curves are depicted in Fig. 6, the ultimate damage maps are illustrated in Fig. 7, and the main parameters and results are also given in Table 2.

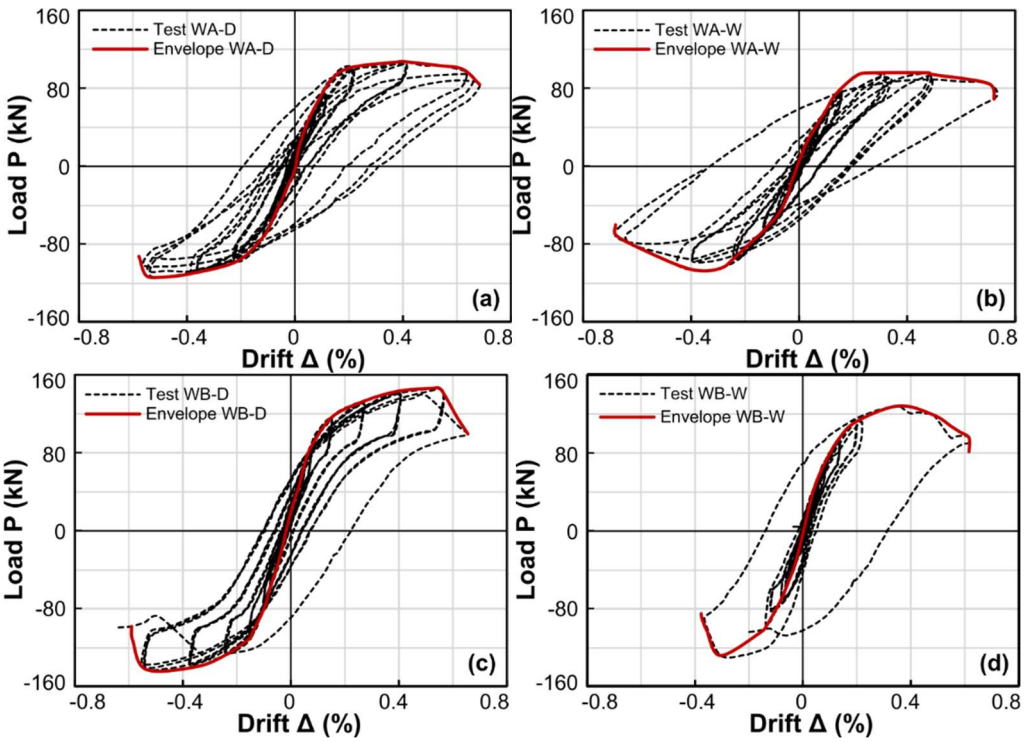

Fig. 6 – Lateral load - drift response of the large-scale walls: a) WA-D, b) WA-W, c) WB-D, d) WB-W

The response of the first ambient-dry wall, Specimen WA-D, was largely symmetric in both loading directions up to about 90% of the peak load, with an initial stiffness K_0 = 86.3 kN/mm. This initial stiffness corresponds to the slope of the line connecting the positive and negative extreme points in the first cycle. The maximum

lateral load carrying capacity was P_{u+}=107.1 kN and P_{u-}=-114.1 kN, respectively. As shown in Fig. 6a, this corresponded to a drift at peak of Δ_{peak+}=0.40% and Δ_{peak-}=0.50% in the push (positive) and pull (negative) cycle, respectively. The overall behaviour was largely governed by shear with no notable sign of flexural bed joint opening. The ultimate failure patterns in Fig. 7a, indicate that the failure was largely due to diagonal tension. Failure was characterised by sliding of the two bodies separated by the diagonal crack following each loading direction. The ultimate drifts corresponding to a 20% reduction in capacity were Δ_{u+}=0.67% and Δ_{u-}=0.58% in the positive and negative cycle, respectively.

The initial stiffness and maximum lateral load carrying capacity, in the positive and negative directions of Specimen WA-W, were K_0=66.6 kN/mm, P_{u+}=95.9 kN and P_{u-}=-107.2 kN, respectively. This corresponded to a drift Δ_{peak+}=0.48% and Δ_{peak-}=0.35% in the push (positive) and pull (negative) cycle, respectively. Compared to its dry counterpart, the wet Specimen WA-W had a less symmetric overall load-drift response, particularly in the post-cracking regime. As indicated in Fig. 6b, the ultimate drifts were slightly different for the two directions. The first visible diagonal crack occurred in the second positive (push) cycle at a drift level Δ=0.30%. The diagonal crack closed during unloading. As for its dry counterpart, the behaviour was largely governed by shear with minimum influence from flexure, with failure eventually occurring due to diagonal tension, as shown by the final crack patterns in Fig. 7b.

The complete load-drift (P-Δ) curve of the air-dry Specimen WB-D and its envelope are illustrated in Fig. 6c and the failure patterns are shown in Fig. 7c. The lateral deformation at peak corresponded to a drift of Δ_{peak+}=0.53% and Δ_{peak-}=0.53% in the push (positive) and pull (negative) cycle. The response of the specimen was largely symmetric in both loading directions with an elastic stiffness K_0=76.9 kN/mm. The corresponding maximum lateral load carrying capacity was P_{u+}=146.3 kN and P_{u-}=142.2 kN, respectively. The transition between elastic and inelastic stiffness occurred at a lateral load (P) around 80 kN in both loading directions. This corresponded to a drift ratio of about Δ=0.1% and was associated with initial signs of cracking. At the third displacement cycle in the positive direction, the specimen failed and was unable to reach the load attained in the previous cycles. Failure was characterised by crushing at the toe and sliding of the two bodies separated by the diagonal crack. The ultimate drifts, assumed to correspond to 20% reduction in load carrying capacity, were Δ_{u+}=0.61% and Δ_{u-}=0.58%.

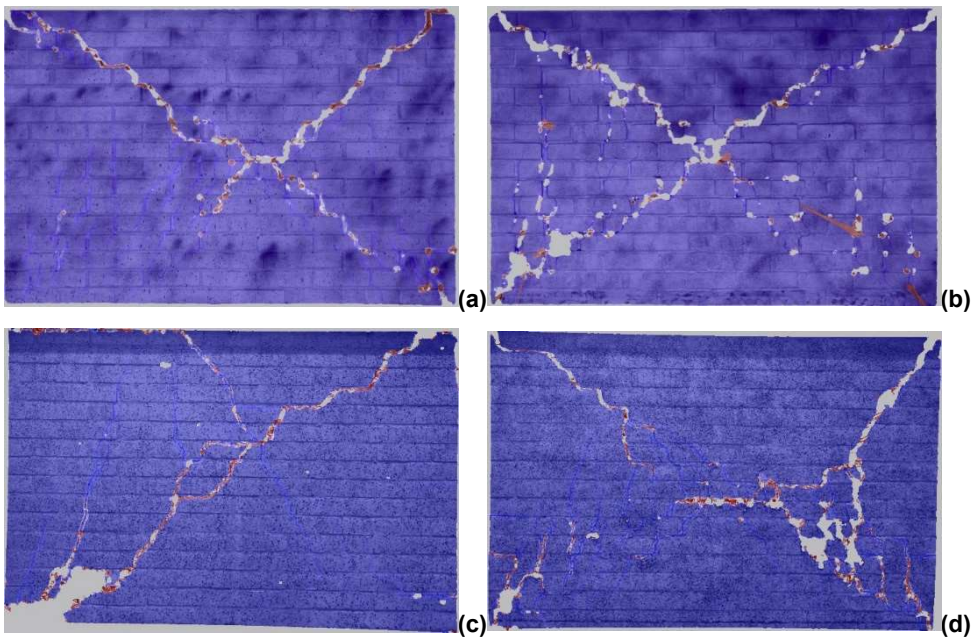

Fig. 7 – Failure characteristics for Specimens: a) WA-D, b) WA-W, c) WB-D, d) WB-W

The full load-drift (P-Δ) and envelope curves of Specimen WB-W are depicted in Fig. 6d, while the crack patterns at failure are shown in Fig. 7d. The response of the specimen was largely symmetric in both loading

directions until about 75% of the peak load. A noticeable reduction in stiffness started at a lateral load of about 35kN (Δ=0.07%) then at 95 kN (Δ=0.25%). The initial stiffness was K_0=75.6 kN/mm. The maximum lateral load carrying capacity was P_{u+}=127.0 kN and P_{u-}=129.2 kN in the two directions. This corresponded to a drift Δ_{peak+}=0.35% and Δ_{peak-}=0.31% in the push (positive) and pull (negative) cycles, respectively. The behaviour of WB-W was initially governed by flexure. The first signs of diagonal cracking were observed at a negative (pull) cycle after Δ=0.20%, with the diagonal crack closing during unloading. At the same drift level in the push (positive cycle), a diagonal crack nearly perpendicular to that occurring from the pull cycle developed, corresponding to the maximum capacity of the specimen. Failure was characterised by sliding of the two bodies separated by the diagonal crack following each loading direction.

Comparing the response of the wet (WA-W and WB-W) and dry (WA-D and WB-D) specimens, the influence of moisture on the stiffness and capacity of the members becomes evident. The average stiffness of the wet specimens was up to 20% lower than the dry walls, whilst the reduction in average lateral strength was up to 11%. These ranges are generally lower both in terms of stiffness and strength, than the differences between wet and dry properties obtained from the diagonal panel tests, due to presence of gravity load. As discussed above, the ductility of the wet walls, in terms of ultimate drift, was broadly similar or lower than that of their dry counterparts, primarily influenced by the post-peak kinematics [13].

Table 2 – Main results from large-scale tests

	Specimen	N (kN)	P_u (kN)	Δ_{peak} (%)	Δ_u (%)	K_{test} (kN/mm)	K_0 (kN/mm)	K_{eff} (kN/mm)	K_{el} (kN/mm)	f_m (MPa)
A	WA-D	227.3	110.6	0.45	0.63	48.6	86.3	45.7	53.6	5.24
	WA-W	225.1	101.6	0.42	0.64	48.9	66.6	41.8	47.1	4.77
B	WB-D	219.9	144.3	0.53	0.60	68.4	76.9	62.0	72.7	6.59
	WB-W	220.7	128.1	0.33	0.47	54.6	75.6	60.5	71.1	6.04

4. Comparative assessments

Based on the test results, the initial stiffness K_0 (slope of line connecting positive and negative extreme points in first cycle), the stiffness K_{test} (within the range of 10-40% of the ultimate capacity), and the effective stiffness K_{eff} from a bilinear idealisation [14], are compared herein with analytical estimates using Eq. 1. Herein, G=0.4×E is assumed as suggested by current design guidelines for masonry structures [15]. The effective stiffness K_{eff} typically varies in the range of 40-80% of the elastic stiffness K_0 and is influenced by the axial load and boundary conditions [16]. In terms of strength, as noted before, all large walls ultimately failed in diagonal tension [17]. The shear capacity for shear-governed conditions, denoted here as V_s and expressed by Eq. 2, uses the Mohr-Coulomb representation, effectively corresponding to the shear-sliding failure mechanism. The guidelines available in the new revision of Eurocode 8 (Part 3) [18], differentiate between shear sliding (V_s) and diagonal cracking (V_d). The shear sliding mechanism has the same formulation as in the current Eurocode 8 (Part 3) (Eq. 2) [9], yet the imposed limit on the maximum shear sliding stress is $0.065f_b$, as a function of the brick compressive strength f_b, rather than that for masonry f_m. Eq. (3) can be used to estimate the diagonal cracking failure capacity.

The diagonal cracking failure mechanism of irregular masonry walls is related to the diagonal tensile strength f_t, which is obtained from diagonal compressive tests such as those described in Sections 2.2 and 3.1 using Eq. (3). The formulation to assess the shear strength of regular masonry walls controlled by diagonal cracking in Eq. 4, related to the formation of stair-stepped cracks, also reverts back to the shear sliding case. However, this is bounded by a limit ($V_{d,lim}$) which is practically of the same form as that of Eq. 3. The parameters f_{v0} and

μ are equivalent shear sliding parameter. The interlocking coefficient φ is defined as the ratio between the height of the brick unit and the length of overlapping between units. The brick tensile strength f_{bt} can be assumed as 10% of the compressive strength f_b. The shear capacity of regular walls is practically the shear sliding capacity bounded by the diagonal tensile cracking failure mode.

$$K_{el} = 1\Big/\left[\left(h^3/\alpha_K EI\right)+\left(h/AG\right)\right] \tag{1}$$

$$V_s = \left(f_{v0} + 0.4\frac{N}{d't}\right)d't \le V_{s,\lim} = 0.065 f_b d't \tag{2}$$

$$V_d = \frac{t\cdot d}{b} f_t \sqrt{1+\frac{\sigma_0}{f_t}} \text{ where } f_t = \frac{P_u}{t\left(d+h\right)} \tag{3}$$

$$V_d = \frac{t\cdot d}{b}\left(\frac{f_{v0}}{1+\mu_j\varphi} + \frac{\mu_j}{1+\mu_j\varphi}\sigma_0\right) \le V_{d,\lim} = \frac{t\cdot d}{b}\frac{f_{bt}}{2.3}\sqrt{1+\frac{\sigma_0}{f_{bt}}} \tag{4}$$

The estimated flexural capacity varied between V_f=121.5-131.0 kN, the sliding shear capacity between V_s=91.4-97.2 kN, whilst the diagonal tension capacity between V_d=102.7-134.4 kN. It can be observed that the governing assessment case would always be the shear sliding. This failure mode was not observed in any of the tests. From a direct comparison between the tests and the estimated shear sliding capacity, the predictions are found to be conservative with V_{test}/V_s=1.29. In contrast, the estimated flexural strengths are generally higher than in the tests, with V_{test}/V_f=0.95, suggesting that it is not the governing failure which is also in agreement with test observations. Finally, the estimated V_d values are found to be closest to V_{test}, when the test material parameters are used. The average V_{test}/V_d ratio is 1.02 with a coefficient of variation of 0.04. This suggests that Eqs. 4 can be used reliably for assessing the diagonal tension capacity of masonry with constituents similar to those described in Section 2.1.

The lateral load-deformation (P-Δ) response of a masonry wall can be represented by an idealised piecewise linear relationship with due account for progressive strength degradation [18]. With reference to Fig. 7, the characteristic points of the relationship can be represented by a bi-linear elastic representation before yield in which the first stage up to 70% of the peak strength (V_u) is a function of the elastic stiffness K_{el}, and the second stage up to V_u is based on 25-50% reduction in K_{el}. In the inelastic regime, a constant slope is assumed between the yield drift Δ_y and ultimate drift Δ_u. The latter corresponds to a drop in the shear force with respect to the peak value, to a 'second' ultimate drift Δ_{u2}, by an amount that depends on the failure mechanism (i.e. flexure, sliding, diagonal tension). Regardless of the failure mode, the 'second' ultimate drift Δ_{u2} is assumed as 4/3 of the ultimate drift Δ_u (i.e. $\Delta_{u2} = 1.33 \times \Delta_u$) [9,18]. According to current seismic assessment guidelines [9], for shear-governed cases, the drift capacity is limited to $\Delta_{v,u}$=0.40%. The revised draft of Eurocode 8 (Part 3) [19] a more detailed procedure to determine the in-plane deformation response. For shear sliding failures of historic (pre-modern) masonry, a value of $\Delta_{s,u}$=0.8% is stipulated, while when shear sliding is limited by masonry unit strength ($V_{s,units}$), $\Delta_{s,u}$=0.5% is suggested, with $\Delta_{s,u2}$=1.33 ×$\Delta_{s,u}$.

The above drift limits suggested by the revised draft of Eurocode 8 [18], along with the predictions of Eqs. (1-3) are used herein to construct the load versus drift response of the large-scale wall specimens. Fig. 7 illustrates a comparative assessment between the test response (V_{test}-Δ_{test}) and the estimated diagonal tension (V_d-Δ_d) response. The drift limits for shear $\Delta_{v,u}$ that conform to the current version of Eurocode 8 [9] are also indicated by vertical lines in the figure. As shown in Fig. 7a-d, the estimated V_d-Δ_d relationships corresponding to diagonal tension failure agree well with the V_{test}-Δ_{test} curves. It is concluded that if the material properties are determined with due account for the strength reduction due to moisture, then Eq. (4) in conjunction with drift parameters in the previous paragraphs of this section can offer a similar level of reliability for the assessment of both wet and dry masonry walls.

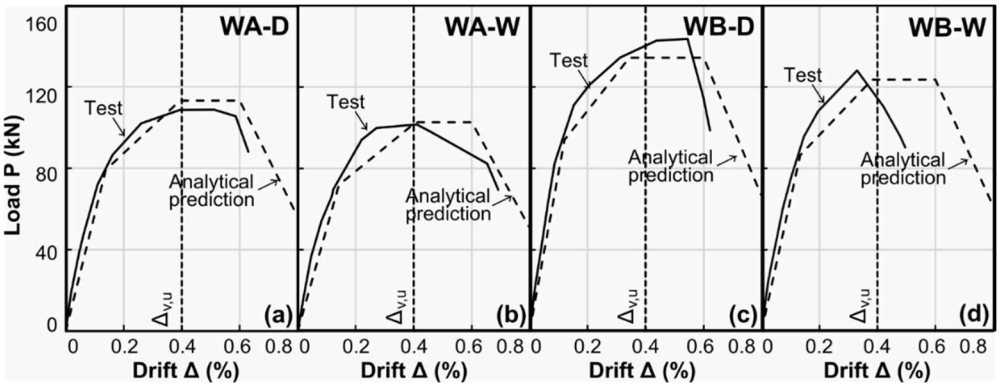

Fig. 8 – Comparative V-Δ curves for Specimens: a) WA-D, b) WA-W, c) WB-D, d) WB-W

5. Concluding remarks

This paper presented an experimental investigation into the material and structural response of ambient-dry and wet clay-brick/lime-mortar masonry elements representative of those in some historic structures. A detailed account of tests on large-scale walls subjected to gravity load and lateral displacements, square panels under diagonal compression, and cylindrical cores in compression, was given. Although, as expected, there is significant inherent variability in the properties of masonry elements, depending on the constituent materials and construction conditions, this investigation offered a detailed insight into the influence of moisture on the behaviour. The extent of moisture effects is a function of the loading conditions and governing behaviour, as a result of several factors, including the relative influence on the brick and mortar mechanical and interaction properties as well as their relative geometry.

A direct comparison between the average load displacement curves of dry and wet masonry specimens tested under diagonal compression showed that moisture reduced both the elastic stiffness and the strength on average by about 35% and 29%, respectively, compared to the dry counterparts. Full-field DIC measurements also showed that the cracking load was reduced by moisture with the brick-to-mortar interface bond loss occurring at around 75% and 85% of ultimate for the wet and dry specimens, respectively. On the other hand, compression tests on cylindrical masonry cores indicated that all uniaxial compression properties were lower when moisture was present. For the configurations tested in this study, the reduction in the elastic modulus and compressive strength was on average in the range of 13.5% and 13.3%, respectively, between the dry and wet cylinders, compared to about 50% reduction in strength due to moisture effects for mortar-only specimens.

For the large-scale masonry walls tested under cyclic lateral loading and typical levels of gravity load, reductions of up to 20% in stiffness and up to 11% in lateral strength were observed in the presence of moisture. All specimens tested under cyclic loading had a brittle failure in diagonal tension with stepped cracks occurring at the two wall diagonals. The ultimate deformations of the wet cyclic walls were either broadly similar or lower than that of the dry counterparts. Considering the ratio of ultimate-to-yield deformation obtained from a bilinear representation as a measure of ductility, the wet walls had ductility drift ratios about 10% lower than those of their dry counterparts.

Finally, analytical assessments related to the performance of large-scale walls indicated that typical estimates for the elastic stiffness were on average about two-third of the initial stiffness obtained in the tests, in agreement with other results from the literature. Importantly, although codified guidance may not be able to predict the failure mode obtained in tests in a realistic manner, their predicted shear capacity of diagonal tension-governed elements was found to be largely reliable. Overall, it was shown that, provided the material properties are determined with due account for the expected strength reduction due to moisture, existing analytical expressions offer a broadly similar level of adequacy for predicting the response of both dry and wet masonry walls.

6. Acknowledgements

The study was carried out within the research project "Interdisciplinary approach for the management and conservation of UNESCO World Heritage Site of Historic Cairo - Application to Al-Ashraf Street" supported by Newton-Mosharafa funding program, a joint fund by the Science, Technology and Innovation Funding Authority (STIFA) of Egypt, Grant No. AHRC30799, and the Arts and Humanities Research Council (AHRC) of the UK Research and Innovation agency, Grant No. AH/R00787X/1. The authors would also like to acknowledge the support provided by the technical staff of the Structures Laboratories at Imperial College London, particularly Mr. P. Crudge, Mr. L. Clark, and Mr. T. Stickland.

7. References

[1] Giaccone D, Santamaria U, Corradi M (2020): An Experimental Study on the Effect of Water on Historic Brickwork Masonry. *Heritage*, **3** (1), 29-46.

[2] Mazzotti C, Sassoni E, Pagliai G (2014): Determination of shear strength of historic masonries by moderately destructive testing of masonry cores. *Construction and Building Materials*, **54**, 421-431.

[3] Bompa DV, Elghazouli AY (2021): Shear-compression failure envelopes for clay brick lime mortar masonry under wet and dry conditions. *PROHITECH 2020*, Athens, Greece

[4] Pelà L, Kasioumi K, Roca P (2017): Experimental evaluation of the shear strength of aerial lime mortar brickwork by standard tests on triplets and non-standard tests on core samples. *Engineering Structures*, **136**, 441-453.

[5] Bompa DV, Elghazouli AY (2020): Experimental and numerical assessment of the shear behaviour of lime mortar clay brick masonry triplets. *Construction and Building Materials*, **262**, 120571

[6] Koutas L, Bousias SN, Triantafillou TC (2014): Seismic strengthening of masonry-infilled RC frames with TRM: Experimental study. *Journal of Composites for Construction*, **19** (2), 04014048.

[7] Sathiparan N, Rumeshkumar U (2018): Effect of moisture condition on mechanical behavior of low strength brick masonry. *Journal of Building Engineering*, **17**, 23-31.

[8] Bompa DV, Elghazouli AY (2020): Compressive behaviour of fired-clay brick and lime mortar masonry components in dry and wet conditions. *Materials and Structures*, **53**, 60,

[9] Eurocode 8. Design of Structures for Earthquake Resistance. Assessment and Retrofitting of Buildings. *EN 1998-3: 2005.* European Committee for Standardization, Brussels, Belgium.

[10] Elghazouli, A. (2016): *Seismic design of buildings to Eurocode 8*. CRC Press.

[11] Lozincă E, Popa V, Coțofană D, Cheșcă AB (2016): Unidirectional Cyclic Behavior of Old Masonry Walls in Romania. *The 1940 Vrancea Earthquake. Issues, Insights and Lessons Learnt,* Bucharest, Romania

[12] Magenes G, Morandi P, Penna A (2008): D 7.1 c Test results on the behaviour of masonry under static cyclic in plane lateral loads. *Test Report, ESECMaSE Poject*, University of Pavia, EURCENTRE, Italy.

[13] Elghazouli AY, Bompa DV, Mourad SA, Elyamani A (2021): Structural behaviour of clay brick lime mortar masonry walls under lateral cyclic loading in dry and wet conditions. *PROHITECH 2020*, Athens, Greece

[14] Salmanpour AH, Mojsilović N, Schwartz J (2015): Displacement capacity of contemporary unreinforced masonry walls: an experimental study. *Engineering Structures*, **89**, 1-16.

[15] Magenes G, Galasco A, Penna A, Da Paré M (2010): In-plane cyclic shear tests of undressed double leaf stone masonry panels. *14th European Conference on Earthquake Engineering,* Ohrid, Republic of Macedonia.

[16] Bosiljkov VZ, Totoev YZ, Nichols JM (2005): Shear modulus and stiffness of brickwork masonry: An experimental perspective. *Structural Engineering and Mechanics*, **20** (1), 21-43.

[17] Elghazouli AY, Bompa DV, Mourad SA, Elyamani A (2021): In-plane lateral cyclic behaviour of lime-mortar and clay-brick masonry walls in dry and wet conditions. *Bulleting of Earthquake Engineering,*

[18] Eurocode 8: Design of structures for earthquake resistance – Part 3: Assessment and retrofitting of buildings and bridges. *Final Document EN1998-3 NEN SC8 PT3. Working draft 2018-05-22.* European Committee for Standardization, Brussels, Belgium.

